Applied Catalysis B: Environmental 147 (2014) 698–710

Contents lists available at ScienceDirect

Applied Catalysis B: Environmental

journal homepage: www.elsevier.com/locate/apcatb

NH_3 formation over a lean NO_X trap (LNT) system: Effects of lean/rich cycle timing and temperature

Christopher D. DiGiulio [a], Josh A. Pihl [b], Jae-Soon Choi [b], James E. Parks II [b], Michael J. Lance [c], Todd J. Toops [b,**], Michael D. Amiridis [a,*]

[a] University of South Carolina, Department of Chemical Engineering, Columbia, SC 29208, USA
[b] Fuels, Engines and Emissions Research Center, Oak Ridge National Laboratory, Oak Ridge, TN 37831, USA
[c] High Temperature Materials Laboratory, Oak Ridge National Laboratory, Oak Ridge, TN 37831, USA

ARTICLE INFO

Article history:
Received 12 April 2013
Received in revised form 7 September 2013
Accepted 11 September 2013
Available online 20 September 2013

Keywords:
NO reduction
Lean NO_X trap (LNT)
Selective catalytic reduction (SCR)
LNT-SCR
NH_3 formation

ABSTRACT

A commercial lean NO_X trap (LNT) catalyst containing Pt, Pd, Rh, BaO, and CeO_2 was evaluated in this investigation. The effects of lean/rich cycle timing on the NO_X, CO and C_3H_6 conversions and on the NH_3 and N_2O selectivities were considered. Two distinct lean/rich cycling regimes were identified. At low temperatures, NO_X release and reduction were relatively slow processes. As a result, a longer, lower-concentration rich dose favored increased cycle averaged NO_X conversions. For example, extending the rich period from 5 to 15 s at 250 °C, while holding the overall reductant dose constant, resulted in an increase in cycle averaged NO_X conversion from 59 to 87%. At high temperatures, the opposite was found to be true. Above 450 °C, NO_X release and reduction occurred very rapidly and shorter, higher concentration rich doses yielded significantly higher NO_X conversions. For example, extending the rich period from 5 to 15 s at 500 °C, while holding the overall rich dose constant, resulted in a decrease in the cycle averaged NO_X conversion from 76 to 54%. The selectivities to NH_3 and N_2O were found to be primarily a function of temperature, with both being higher at lower temperatures. The effect of cycle timing and reductant concentration were of secondary importance. In contrast, NH_3 and N_2O yields were significantly affected by the cycle timing since they depend on the NO_X conversion. Therefore, any combination of changes in the lean/rich timing protocol or reductant concentrations that resulted in increased NO_X conversion also resulted in increased NH_3 and N_2O yields for a given temperature. Thus, concerted control of NH_3 generation by varying the lean/rich cycle timing was demonstrated for this LNT catalyst. At both lower and higher temperatures, variations in the rich cycle duration resulted in NH_3/NO_X ratios that could extend the region of operation for a close-coupled LNT-SCR system, with the greatest effect observed at temperatures between 250 and 450 °C. However, N_2O yield also increased with NH_3 yield under the same conditions.

1. Introduction

Lean-burn engines are more fuel efficient and produce less overall CO_2 per mile when compared to stoichiometric-burn engines. However, meeting NO_X emission regulations for lean-burn engines through the use of advanced catalytic converter technologies still represents a significant technical challenge. Over the past 15 years, lean NO_X trap (LNT) [1] and selective catalytic reduction (SCR) [2] catalysts have been identified as two promising systems for the removal of NO_X from the exhausts of lean-burn engines. In several recent publications and patents, there has been considerable discussion regarding the advantages of combining these two technologies into a coupled LNT-SCR system [3–23]. As a brief review, LNTs are designed to function under periodic lean/rich environments, where NO_X is stored in the form of nitrites or nitrates on a storage component (e.g., Ba) during lean periods typically lasting 60–120 s [1,24]. As time elapses, the storage component becomes saturated with NO_X and a subsequent rich step, typically lasting 1–5 s, must be employed to reduce the stored NO_X and in the process regenerate the storage component. Catalytic formulations used commercially generally include platinum group metals (PGM; e.g., Pt, Pd and Rh) supported on a BaO and CeO_2-modified γ-Al_2O_3 [1]. While N_2 is obviously the most desirable product during NO_X reduction, NH_3 and N_2O can also be formed and under certain conditions, the selectivity to these undesirable by-products can be significant. For example, Ren and Harold [25]

* Corresponding author. Tel.: +1 803 7772808; fax: +1 803 7779502.
** Corresponding author. Tel.: +1 865 9461207; fax: +1 865 9461354.
E-mail addresses: toopstj@ornl.gov (T.J. Toops), amiridis@cec.sc.edu (M.D. Amiridis).

0926-3373/$ – see front matter © 2013 Elsevier B.V. All rights reserved.
http://dx.doi.org/10.1016/j.apcatb.2013.09.012

reported selectivities to NH_3 of 40%, or greater, for a series of model LNT catalysts operating below 200 °C. At similar temperatures, Bonzi et al. [13] attributed the high selectivity to NH_3 to a combination of significant NH_3 formation and slow subsequent reaction of the NH_3 formed with the remaining stored nitrites/nitrates. This reaction becomes significantly faster at higher temperatures, thus contributing to reduced NH_3 selectivities. While NH_3 formation over the LNT catalyst is undesirable in a single catalyst system, it also clearly demonstrates the potential for a coupled LNT-SCR configuration.

In contrast to LNT catalysts, NH_3-SCR catalysts are operated under steady-state conditions and were originally designed for use in stationary applications [26,27]. Current commercial SCR catalytic formulations include V_2O_5–WO_3/TiO_2 or Cu/Fe exchanged zeolites [26,27], with the zeolite-based materials favored for automotive applications due to their lower temperature activity, as well as their ability to store significant amounts of NH_3 under transient conditions [28,29]. Initially, commercialization of zeolite-based SCR catalysts was limited due to hydrothermal stability issues, but recent advances in this area have led to the development of hydrothermally stable Cu-zeolite catalysts that are active over a broad temperature range [28,30]. Zeolites are particularly attractive for a coupled LNT-SCR configuration because of their ability to store NH_3 generated over the LNT catalysts during short rich cycles, which is stable under lean conditions. NH_3 thus stored can be used in the subsequent lean cycle to reduce NO_X that is not trapped by the LNT catalyst. As outlined by Bonzi et al. [13], the LNT-SCR configuration has the advantage of both increasing the selectivity to N_2 and the overall NO_X conversion when compared to a single LNT system. For example, Lindholm et al. [22] reported a cycled averaged NO_X conversion of 99.5% for an LNT-SCR system operating at 300 °C, but also observed increases in the NO_X conversion and N_2 selectivity over the entire temperature range (200–400 °C) investigated when compared to a single LNT system. Similarly, Xu et al. [18] recently reported that LNT-SCR systems have the additional benefit of requiring a lower PGM content for the LNT, increasing the temperature window for high NO_X conversion and mitigating catalyst deactivation due to aging. In summary, a consensus has emerged that addition of an SCR catalyst, either in series, as a physical mixture or in a layered geometry, to an LNT exhaust system can result in significant improvements in overall catalytic performance. However, the majority of these investigations have either been performed under typical LNT cycling conditions (e.g., 60 s lean, 5 s rich) or under extended isothermal step conditions and the role of cycle timing has not been investigated in detail. Furthermore, while a number of investigations [31–37] have reported NH_3 formation over LNT catalysts – either as an undesirable byproduct or as an intermediate in the reduction mechanism – the concerted use of an LNT catalyst for NH_3 formation by optimization of the cycle timing, catalyst temperature, or reductant concentration, has not been considered. Such an approach could potentially lead to a more effectively coupled LNT-SCR system. This is different from recent investigations using LNT-SCR systems [3–23] because in those cases the SCR catalyst is added to take advantage of NH_3 that is inevitably formed as a result of typical lean/rich cycling over the LNT catalyst. The proposed strategy is expected to result in a more efficient LNT-SCR system since the amount of NH_3 formed could be optimized to match the amount of unreacted NO_X, hence, creating optimal conditions for the operation of the downstream SCR catalyst.

In this manuscript, the role of both lean and rich LNT cycle timing is addressed with specific emphasis placed on the amount of NH_3 generated in relation to the amounts of NO_X and CO slip from the LNT catalyst. In addition, N_2O formation was closely monitored under these conditions. Finally, the concept of concerted control of the NH_3 generation by the control of cycle timing and conditions is introduced with the goal of more effectively optimizing the LNT-SCR system.

2. Experimental

2.1. Catalytic material

A fully formulated LNT monolith (wash-coated honeycomb cordierite monolith removed from a Lean-GDI, BMW 120i, Model Year 2009) was utilized in the present investigation. On the vehicle, the LNT catalyst brick of 413 cell per square inch (cpsi) is used in an under-floor configuration. The catalyst has now been adopted as the new representative commercial LNT catalyst in the Crosscut Lean Exhaust Emissions Reduction Simulations (CLEERS) research community [38].

2.2. Catalyst characterization

Semi-quantitative metals screening of the LNT catalyst using inductively coupled plasma-mass spectrometry (ICP-MS) was conducted by Galbraith Laboratories, Inc. (Knoxville, TN). Inductively coupled plasma-atomic emission spectroscopy (ICP-AES), which afforded quantitative results, was also conducted by Galbraith Laboratories, Inc.

A JEOL JXA-8200 SuperProbe Electron Probe MicroAnalyzer (EPMA) was used to map the elemental composition of the catalyst washcoat. Samples were prepared for imaging by mounting them in epoxy and polishing. The spot size was approximately one cubic micron, which is smaller than the typical grain size of the constituent phases. A Hitachi 4800 field emission gun scanning electron microscope (FEG-SEM) with an EDAX energy dispersive spectroscopy (EDS) X-ray detector was also used to measure the elemental composition of individual grains. Since the sample was heterogeneous and porous, no attempt was made to calibrate the X-ray intensities with standard samples. Therefore the compositional data is likely accurate to no less than one percent and should be viewed more as a relative comparison between different grains in the wash coat.

2.3. Catalytic evaluation

Lean/rich cycling was performed using a laboratory bench-flow reactor, as described in more detail elsewhere [39,40]. Briefly, the LNT monolithic core (2.1 cm wide × 5.5 cm long; SV = 30,000 h^{-1}; ≈9150 standard cm^3/min) was tightly wrapped in Zetex insulation tape and inserted into a horizontal quartz tube reactor. The reactor was heated using a horizontal bench-top furnace (Lindberg/Blue M). Lean/rich gas mixtures were prepared using pressurized gas cylinders (UHP, Air Liquide) and a system of mass flow controllers (Unit Instruments Series 7300, Kinetics Electronics). A rapid switching 4-way valve system was used to alternate between the lean and rich gas mixtures. Water was introduced using a peristaltic pump (Cole-Parmer) that fed into a heated, flash-vaporization zone held at 350 °C. All gas lines downstream of the water introduction zone were heated, and quartz chips were placed upstream of the monolithic core to ensure that the feed gas temperature reached the set point temperature prior to contacting the catalyst. Three thermocouples were used to measure the temperature. The first was placed 1 cm upstream of the core and was used to record the inlet/set-point temperature. The second thermocouple was placed in the middle of the monolithic core and was used to record the actual monolith temperature. The third was placed 1 cm downstream of the core and was used to record the temperature exiting the core. After exiting the reactor, the gas was fed to an MKS MultiGas™ 2030 HS FT-IR analyzer, which allowed for continuous tracking (5 Hz) of NO, NO_2, N_2O, NH_3, CO, C_3H_6, CO_2

and H_2O concentrations. Prior to the reactor measurements, the as-received catalyst was "de-greened" at 700 °C in a 10% H_2O/air mixture for 16 h to establish reproducible performance. Unless otherwise denoted, all calculations were performed using the last 4 cycles obtained during lean/rich cycling, where Eqs. (1)–(3) were used to calculate the cycle averaged NO_X, CO and C_3H_6 conversion, respectively.

$$X_{NO_X} = \frac{\int NO_{X_{Fed}} - \int NO_{X_{Slipped}}}{\int NO_{X_{Fed}}} \times 100 \quad (1)$$

$$X_{CO} = \frac{\int CO_{Fed} - \int CO_{Slipped}}{\int CO_{Fed}} \times 100 \quad (2)$$

$$X_{C_3H_6} = \frac{\int C_3H_{6_{Fed}} - \int C_3H_{6_{Slipped}}}{\int C_3H_{6_{Fed}}} \times 100 \quad (3)$$

Eqs. (4)–(7) were used to calculate the NH_3 and N_2O yields and selectivities, respectively. The total amount of products formed was calculated based on the total amount of NO_X consumed. Since N_2 formation could not be quantified by the FTIR analyzer, the N_2 yield and selectivity was calculated using a nitrogen mass balance by assuming that NH_3, N_2O, and NO_X were the only nitrogen containing by-products formed.

$$Y_{NH_3} = \frac{\int NH_{3_{Produced}}}{\int NO_{X_{Fed}}} \times 100 \quad (4)$$

$$S_{NH_3} = \frac{\int NH_{3_{Produced}}}{\int NO_{X_{Fed}} \times X_{NO_X}} \times 100 \quad (5)$$

$$Y_{N_2O} = \frac{2 \times \int N_2O_{Produced}}{\int NO_{X_{Fed}}} \times 100 \quad (6)$$

$$S_{N_2O} = \frac{2 \times \int N_2O_{Produced}}{\int NO_{X_{Fed}} \times X_{NO_X}} \times 100 \quad (7)$$

A total of 81 sets of conditions were considered in this investigation, consisting of combinations of nine temperatures (150–550 °C, in 50 °C increments) and nine different cycle timing protocols. The lean period gas concentration was held constant at 500 ppm NO, 8% O_2, 5% H_2O and 5% CO_2 in N_2. The rich period included a variable amount of reductants with a balance of 5% H_2O and 5% CO_2 in N_2. The required amount of reductants (i.e., H_2, CO and C_3H_6) in the rich dose was calculated by adding the stoichiometric amount of reductant required to completely reduce all of the NO_X fed plus the required amount of reductants required to consume all of the O_2 storage capacity of the LNT catalyst, as shown more clearly in Eq. (8) below.

$$\mu\text{moles reductant required} = \mu\text{moles CO consumed in OSC measurement} + \mu\text{moles } NO_X \text{ fed} \quad (8)$$

The amount of CO consumed due to the oxygen storage capacity (OSC) on the LNT catalyst was measured by cycling (60 s lean/5 s rich) in a lean gas mixture comprised of 10% O_2, 5% H_2O and 5% CO_2 in N_2 and a rich gas mixture comprised of a variable concentration of CO, 5% H_2O and 5% CO_2 in N_2. The CO concentration was adjusted during this cycling (in 0.1% increments) until consistent breakthrough of CO was observed (by FT-IR analyzer and lambda sensor), indicating that all of the available O_2 present on the LNT catalyst had been consumed. This procedure is similar to the one previously described by Boaro et al. [41]. Table 1 displays the required CO concentrations necessary to reduce the OSC of the LNT catalyst used as a function of temperature. For temperatures below 300 °C, a value of 1.6% was assumed since complete O_2 consumption required longer times than provided in the 5 s rich period and accurate measurements could no longer be obtained.

Table 1
CO concentration required to consume the OSC of the LNT catalyst at different temperatures.

Temperature (°C)	OSC (CO %)
350	1.6
400	1.6
450	1.7
500	1.7
550	1.7

Table 2
Calculated reductant concentrations for the cycle timing protocols used in this investigation in the 150–400 °C range (OSC = 1.6% CO).

Lean/rich timing (s)	Reductant concentrations		
	CO (%)	H_2 (%)	C_3H_6 (%)
60/5	2.01	0.67	0.112
60/10	1.01	0.34	0.056
60/15	0.67	0.22	0.037
120/5	2.83	0.94	0.157
120/10	1.42	0.47	0.079
120/15	0.94	0.31	0.052
180/5	3.65	1.22	0.203
180/10	1.82	0.61	0.101
180/15	1.22	0.41	0.068

The calculated rich dose (i.e., the total number of moles of reductant required) was then held constant and the rich cycle duration was varied. Therefore, shorter rich cycle times (e.g., 5 s) contained higher concentrations of reductants, while longer rich cycle times (e.g., 10 and 15 s) contained lower concentrations of reductants. Once the total amount of reductants needed was determined, their relative concentrations were calculated based on a 18:6:1 ratio for $CO:H_2:C_3H_6$, respectively. This ratio is considered to be representative of rich engine exhaust [42].

Table 2 shows the calculated reductant concentrations for different cycling times for an OSC corresponding to 1.6% CO. As shown in the Table, these concentrations varied both with the lean cycle timing (since the total amount of NO_X fed varies in this case) and rich cycling timing (since the total amount of reductants fed has to remain constant regardless of the length of the rich period). Slightly higher concentrations were used at temperatures above 450 °C due to the increase in the OSC to 1.7% CO (not shown for brevity).

3. Results and discussion

3.1. Catalyst characterization

Semi-quantitative inductively coupled plasma-mass spectrometry (ICP-MS) analysis of the LNT catalyst indicated the presence of Mg, Al, Ce, and Ba as major components. Other elements of significance included Zr, La, Pt, Pd, and Rh. The results of inductively coupled plasma-atomic emission spectroscopy (ICP-AES) also indicated the presence of Pt, Pd, Rh, Ba, Ce, Zr, and La on the LNT catalyst used. The loadings of these elements are summarized in Table 3.

The washcoat is composed of three separate layers of roughly equal thickness, indicating that three separate dip coats were applied during processing. The presence of mud-cracks, normal to the substrate surface as seen in Fig. 1 and ending at the layer interfaces, further indicates that three separate drying steps were also performed during processing. The elemental composition of these

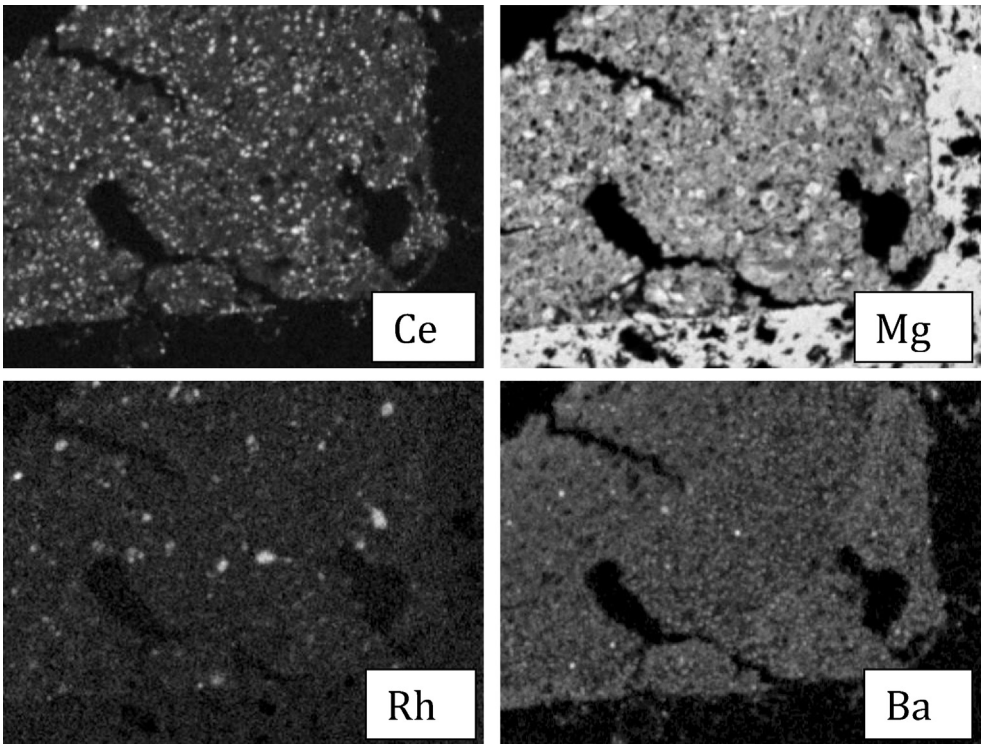

Fig. 1. EPMA maps for Ce, Mg, Rh and Ba in a washcoat corner of the front section of the LNT catalyst brick.

Table 3
Elemental composition of the LNT catalyst used in this investigation.

	Lean GDI, BMW 120i (2009) Loading[a] (g/L)
Pt	2.2
Pd	0.8
Rh	<0.3[b]
Total PGM (g/L)	3.3[b]
PGM ratio (Pt/Pd/Rh)	7/3/1[b]
Ba	19.9
Ce	55.5
Zr	4.3
La	2.5

[a] The relative error of the ICP-AES results used for the loading value estimation (at 95% confidence) was estimated at: ±8% for Pd; ±9% for Pt and Zr; ±15% for Ce; ±16% for Ba; and ±24% for La.

[b] The Rh content was lower than the quantitation limit of the ICP-AES measurements performed. Semi-quantitative ICP-MS measurements estimated Rh loading between 0.1 and 0.3.

three layers appears to be identical. The total washcoat thickness ranges from 79 ± 10 μm at the side of the channel to 270 ± 24 μm at the channel corner.

We can discern four compositionally distinct domains from EPMA maps of Ce, Mg, Rh, and Ba in Fig. 1: a CeO_2 phase with low amounts of La, Zr, Pt, Pd, and Ba (Ce/Zr mixed oxide domain); a Mg/Al oxide spinel phase with some Ce, Pd, and Ba (Mg/Al mixed oxide domain); in a few spots, an Al_2O_3 phase with Rh, as well as some Pd and Ba present (Al oxide domain); and grains rich in Ba. Generally, the number of Ba-rich grains appeared to be rather limited, which may indicate a more uniform Ba dispersion in this LNT catalyst in comparison to a different LNT catalyst formulation considered in previous investigations [39,40]. Indeed, the Ba map (Fig. 1) shows a uniform distribution of Ba over the entire washcoat cross-section. The compositions of the Ce/Zr and coarse-grained Mg/Al mixed oxide domains measured with EDS are shown in Fig. 2. As discussed in the experimental section however, no attempt was made to calibrate the X-ray intensities with standard samples and the results shown in Fig. 2 are included as a semi-quantitative comparison between different grains in the wash coat. The Mg/Al mixed oxide domain exhibits a bimodal grain size distribution with large 5–10 μm grains interspersed with submicron-sized grains.

3.2. Representative lean/rich cycling over the LNT catalyst

Reactor effluent concentrations observed at 300 °C during 60 s lean/5 s rich cycling over the LNT catalyst used in this investigation are shown in Fig. 3 as a representative example for the performance of this catalyst. As expected, low concentrations of NO_X were observed during the lean period indicating that the majority of NO_X was stored on the LNT catalyst. As the reactor feed was switched to the rich mixture (after 60 s) and the regeneration of the LNT catalyst was initiated, a significant un-reacted NO_X release was observed simultaneously with the formation of N_2O. Previous literature reports have addressed both of these observations [40,43–48], with the NO_X release attributed to the slower NO_X

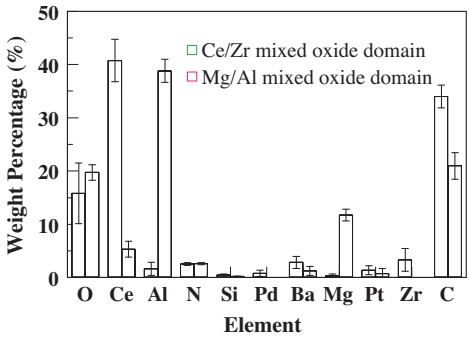

Fig. 2. Elemental compositions in weight percentage of the two primary phases in the LNT catalyst washcoat, as measured by EDS (carbon signal originating from the mounting epoxy).

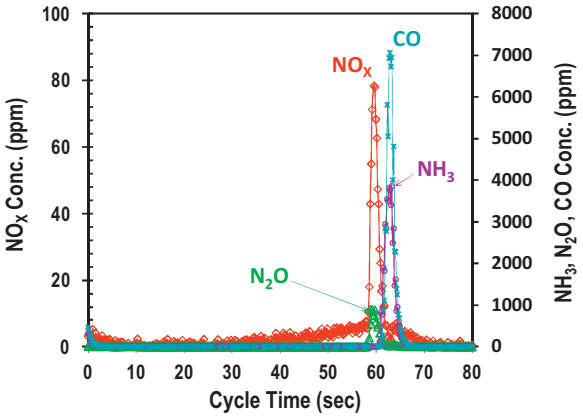

Fig. 3. Effluent concentrations of NO_X, N_2O, NH_3 and CO observed at 300 °C over the LNT catalyst as functions of cycle time during a 60 s lean/5 s rich cycling run.

reduction kinetics at this temperature in comparison to the surface nitrite/nitrate decomposition [43,44] and the N_2O formation linked to the relative concentrations of surface NO and N intermediates present [40,43–48]. The amount of NO_X release at the interface of lean/rich cycles has also been shown to depend to the amount NO_X stored on the LNT, the temperature, the rich A/F ratio, the aging condition of the LNT, the flowrate, and the catalyst formulation [49]. Subsequent formation and breakthrough of NH_3 and CO were also observed during the rich cycle, with an approximately 2.5 s delay between the onset of the rich cycle and the appearance of these products in the reactor outlet. The delay for NH_3 has previously been attributed to the reaction of NH_3 formed upstream on the LNT catalyst with downstream surface nitrites/nitrates and oxygen stored on the catalyst [32,35,48,50,51]. Likewise, the delay in CO breakthrough is most likely a combination of several contributing factors including the amount of CO reacting with stored NO_X and oxygen, as well as its participation in the water gas shift reaction (WGS). The near-simultaneous appearance of CO and NH_3 in the reactor outlet during reduction is an important feature of the LNT catalyst behavior in light of its potential use in an LNT-SCR configuration. While NH_3 could be stored in the SCR material, CO storage and/or oxidation over the downstream SCR catalyst under rich conditions is highly unlikely. Therefore, for practical implementation of the LNT-SCR technology, the amount of CO slip from the LNT catalyst needs to be closely monitored as a function of operating conditions and or catalytic formulation and eventually converted to CO_2.

Table 4 summarizes the performance of the LNT catalyst at 300 °C (60 s lean/5 s rich) and provides corollary results calculated from the results shown in Fig. 3. The majority of NO_X fed to the reactor during the lean cycle is stored and reduced during the subsequent rich step, resulting in a cycle averaged NO_X conversion of 99.2%. Interestingly, the selectivity to N_2 for this cycle timing protocol and temperature is fairly low (59.2%), in agreement with other investigations conducted under similar conditions [25,43]. A significant percentage of the stored NO_X (29.0%) reacted to form NH_3, where the NH_3 production is approximately 62 μmol/cycle, while the total amount of NO_X slip is only 1.6 μmol/cycle. The difference between the amount of NH_3 produced and NO_X slip as well as the difference in time evolution of the two species demonstrate the need for NH_3 storage on the SCR, since equimolar formation of NH_3 to match the amount of NO_X slipped would be expected to result in improved LNT-SCR operation. The selectivity to N_2O was also high (11.8%) under these conditions, while CO and C_3H_6 conversions were relatively low (87.1 and 77.5%, respectively). Once again, we should point out that the data from this cycling condition were included only as a representative example because they demonstrate both the potential advantages and drawbacks of LNT operation under conditions favorable for NH_3 production. In subsequent sections, the NH_3 and N_2O trends will be discussed in more detail.

Table 4
Summary of the cycling performance of the LNT catalyst at 300 °C (60 s lean/5 s rich).

X_{NO_X}	99.2%
X_{CO}	87.1%
$X_{C_3H_6}$	77.5%
NO_X fed (lean)	214.8 μmol/cycle
NO_X stored	214.2 μmol/cycle
NO_X slip (total)	1.6 μmol/cycle
NO_X slip (rich)	1.1 μmol/cycle
NH_3 produced	61.9 μmol/cycle
N_2O produced	12.5 μmol/cycle
Y_{NH_3}	28.8%
Y_{N_2O}	11.7%
S_{NH_3}	29.0%
S_{N_2O}	11.8%
S_{N_2}	59.2%

3.3. Cycle averaged NO_X, CO and C_3H_6 conversions

The results shown in Fig. 4 summarize the cycle averaged NO_X conversions measured in this investigation at different temperatures and under different lean/rich cycle timing protocols. These results indicate that with respect to NO_X conversion the optimum operating temperature for this LNT catalyst is between 350 and 400 °C. Cycling conducted using a 60 s lean period resulted in cycle averaged NO_X conversions over 80% from 300 to 450 °C temperature range. However as the extent of the lean period duration was increased, the temperature window for high NO_X conversion was decreased. As a result, longer lean periods (e.g., 120 and 180 s, respectively) can only be used if the LNT catalyst is operated at, or very near, an optimum temperature of 350–400 °C. For all timing protocols investigated, dramatic decreases in the cycle averaged NO_X conversion were observed at temperatures below 300 °C and above 450 °C. Under such conditions, higher cycle averaged NO_X conversions were observed for longer rich periods in the low temperature regime (i.e., below 300 °C). By contrast at temperatures above 450 °C, the highest cycle averaged NO_X conversions were observed for shorter (5 s) rich periods. The results for two cases (i.e., 250 and 500 °C) are further displayed in Fig. 5, but similar trends were also observed at 300 and 450 °C, as shown in Fig. 4. At 350 and 400 °C, the cycled averaged NO_X conversion was approximately 100% for all of the conditions considered; therefore, discerning the effect of the regeneration duration and/or reductant concentration at these temperatures was not possible.

The results shown in Figs. 4 and 5 can be rationalized considering differences in the relative rates of NO_X release and reduction as a function of temperature. For example, at 250 °C both the NO_X release and its subsequent reduction take place at lower rates, which explains why longer, lower concentration rich doses are more effective. In this case, extending the rich period led to a significant increase in the cycle averaged NO_X conversion from 59 to 87% for a 60 s lean period with 5 and 15 s rich periods, respectively. While the rich period duration was increased, the total number of moles of reductant was held constant, as discussed in Section 2.3. Thus, it becomes apparent that because of the slow NO_X release and/or reduction rates a more extended temporal distribution of the reductants can optimize the NO_X conversion characteristics of the LNT catalyst.

This conclusion is further supported by the results shown in Fig. 6, where the NO_2 reactor effluent profiles are shown for a number of lean cycles at the onset of the catalyst operation. As can be seen in the results, a considerable number of lean/rich cycles

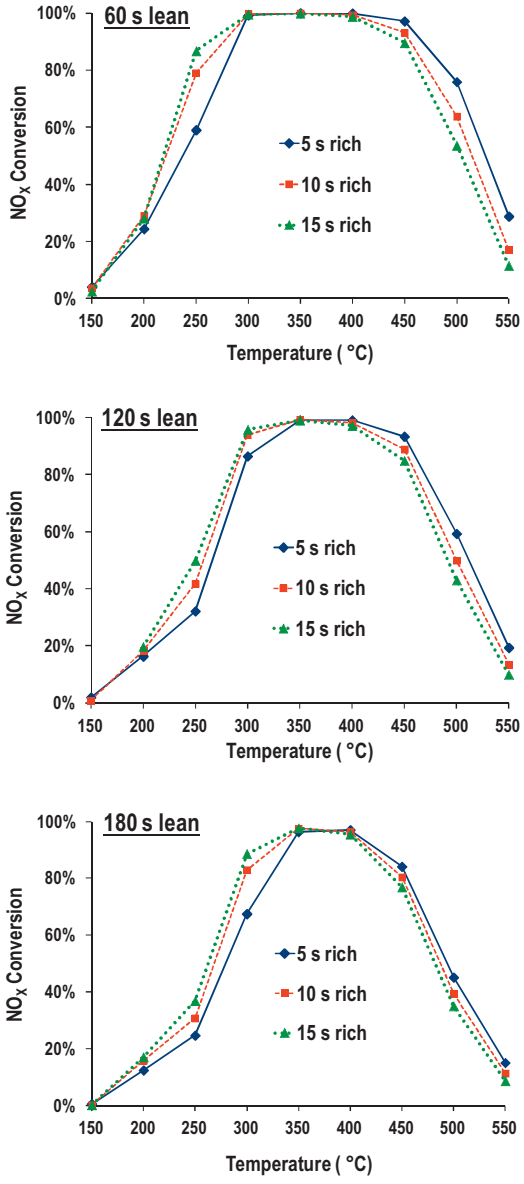

Fig. 4. Cycle averaged NO_X conversions obtained for the LNT catalyst as functions of temperature for different lean/rich cycle timing protocols.

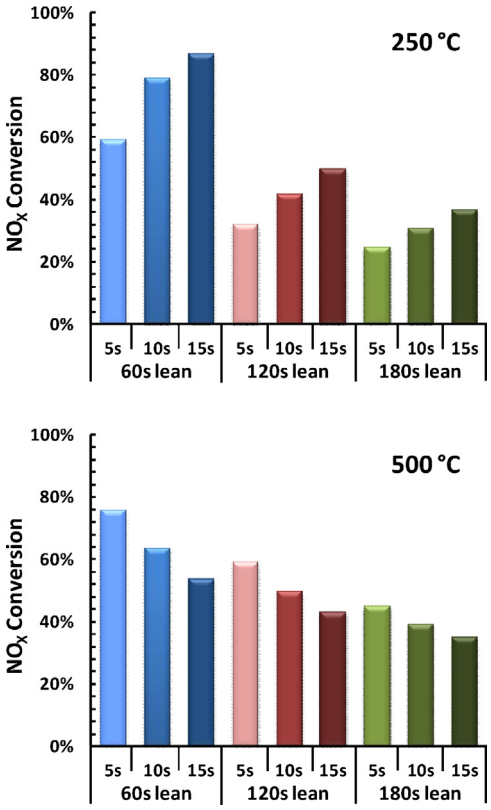

Fig. 5. Cycle averaged NO_X conversions obtained for the LNT catalyst for different lean/rich cycle timing protocols at 250 and 500 °C.

(i.e., ≥30) need to be completed at this temperature before a periodic steady-state is achieved. In the first several cycles, no NO_X is released from the catalyst. However as cycling continues, NO_X breakthrough is observed and the amount of NO_X released per cycle continues to increase until behavior representative of periodic steady-state cycling is observed. The high removal of NO_X during the first few cycles can be attributed to the accumulation of NO_X on the LNT catalyst. Apparently, the capacity of the catalyst is higher than the amount of NO_X introduced during a single 60 s lean cycle and as a result, accumulation continues during subsequent cycles until the full NO_X storage capacity on the LNT catalyst is fulfilled. Once this point has been reached, the cycled-averaged NO_X conversion becomes dependent on the relative rates of NO_X storage, NO_X release and NO_X reduction for the specific set of conditions.

The observed NO_X accumulation on the LNT catalyst at 250 °C is consistent with the results of recent CO-TPSR experiments conducted by Forzatti et al. [52] over a representative LNT catalyst, indicating that NO_X reduction did not begin until 180 °C and complete utilization was not observed until 270 °C. Breen et al. [53] similarly reported that the rate of reduction/regeneration limits the performance of LNT catalysts at 250 °C. Thus, slower rates of regeneration are expected at lower temperatures, especially if cycling is performed below 270 °C. Lastly, the regeneration process, should not be viewed as a single chemical reaction step, since slower rates of surface diffusion of NO_X to the precious metal site and/or of the reducing agents to the stored NO_X sites, have been suggested to limit the efficacy of this process [33,45] at lower temperatures.

At 500 °C, NO_X release and reduction processes are faster and as a result, shorter, high concentration rich doses are needed to effectively reduce the NO_X that is rapidly released from the LNT catalyst. This behavior is not surprising since thermal release of

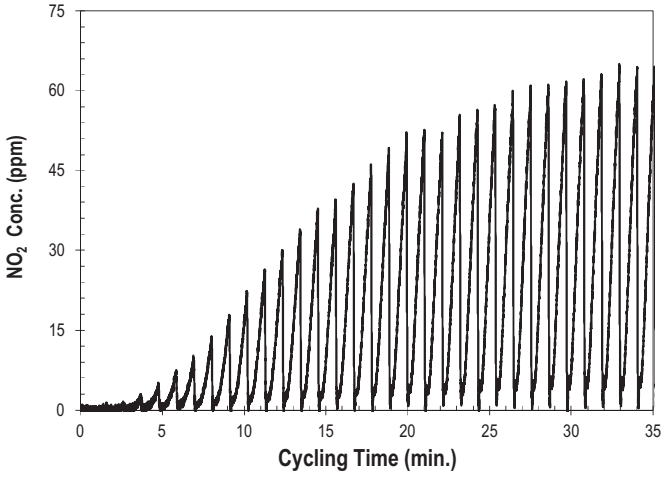

Fig. 6. NO_2 effluent profiles obtained during 60 s lean, 5 s rich cycling over the LNT catalyst at 250 °C.

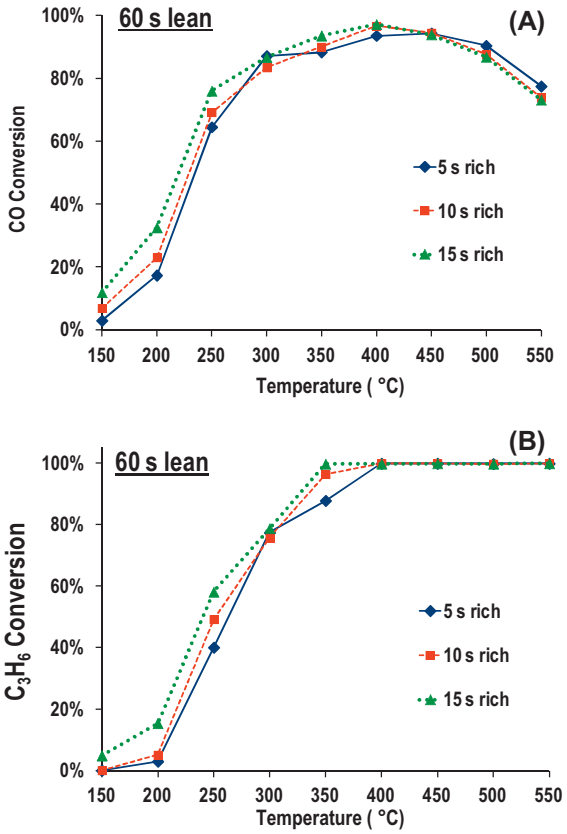

Fig. 7. Cycle averaged CO (A) and C_3H_6 (B) conversions obtained for the LNT catalyst as functions of temperature for different lean/rich cycle timing protocols.

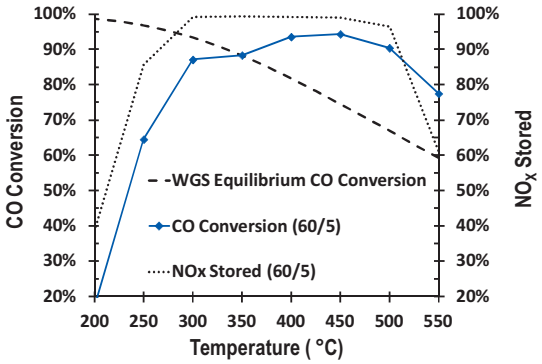

Fig. 8. Cycle averaged CO conversion obtained for the LNT catalyst in comparison to the amount of NO_X stored and the WGS equilibrium conversion as a function of temperature (60 s lean/5 s rich).

NO_X is favored even in the absence of a reducing agent at temperatures exceeding 470 °C for ceria containing LNTs [54]. This is further supported by the observation that the majority of the NO_X that is not reduced during cycling (≥85%) is released during the rich period for temperatures above 400 °C. In summary, longer, lower concentration rich doses result in higher NO_X conversions below 300 °C, while shorter, higher concentration rich doses achieve the same result at temperatures above 400 °C. Breen et al. [55] similarly observed increased NO_X conversions for longer, lower concentration rich doses, but concluded that such timing protocols were always more effective regardless of the operating temperature. Al-Harbi and Epling [56] also observed increased NO_X conversions at 500 °C for shorter rich periods, but the effects in their case was more modest than what was observed over the LNT catalyst used in our study. Ultimately, Al-Harbi and Epling [56] concluded that the simultaneous increase in NH_3 generation for the shorter, higher concentration, rich doses at high temperatures negated the benefits of increased NO_X conversion. However in an LNT-SCR configuration, NH_3 generation can be mitigated by the downstream SCR catalysts and might even be desirable. Lastly, Kabin et al. [57] similarly reported that shorter, higher concentration rich periods led to increased NO_X conversion at 300 °C, which generally agrees with the results presented here for higher temperatures (e.g., 350–500 °C).

The cycle averaged CO and C_3H_6 conversions are shown in Fig. 7. Since both the CO and C_3H_6 conversions were largely insensitive to the cycle timing, only data for the 60 s lean period are shown. In all cases, the LNT catalyst exhibited low CO and C_3H_6 conversions below 200 °C, indicating a low reactivity between these two reductants and NO_X at these temperatures. This is consistent with previous results reported by Abdulhamid et al. [58], which indicate that CO is not as effective as H_2 in reducing NO_X at temperatures below 200 °C. Furthermore, more recent investigations by different groups [24,37,59–61] indicate that hydrolysis of isocyanates and hydrogen production via the WGS reaction exhibit significant activity above 250 °C, which may explain the higher consumption of CO observed in Fig. 7 at these temperatures. However, the most important factor for the higher CO conversions observed in the 300–500 °C temperature range may be the relative amounts of NO_X stored and CO fed, as shown in Fig. 8, since it becomes apparent that at these temperatures, the CO conversion tracks very closely the amount of NO_X stored on the LNT catalyst. Above 500 °C, where the thermal desorption of NO_X becomes thermodynamically favored, the CO conversion is no longer strongly related to the amount of NO_X stored, but it also appears to be affected by the WGS reaction equilibrium conversion, as implied by a comparison of the slopes of the two lines. The results in Fig. 8 suggest that CO may be involved in two parallel reactions; the direct reduction of stored NO_X and the WGS reaction, which yields H_2 that can subsequently reduce stored NO_X. The relative contribution appears to be dependent on the reduction temperature. In addition to these two parallel pathways, CO could also react with oxygen stored on the LNT catalyst in the form of CeO_2, which further complicates the task of decoupling the amount of CO consumed via the reaction with stored NO_X. Alternatively, CO could also be produced by steam reforming of hydrocarbons, which would lower the apparent CO conversion.

The C_3H_6 cycle-averaged conversion curves shown in Fig. 7B resemble typical, steady-state light-off curves although the data were collected under cycling conditions. Once again, the differences due to the length of the rich cycle are minimal. In the absence of H_2O, Abdulhamid et al. [58] reported that propylene shows limited activity toward the reduction of NO_X when compared to CO and H_2 at 250 °C, but similar activity with the other two reductants at 350 °C. Theis et al. [62] also reported H_2 to be a much more effective reductant when compared to CO and C_3H_6. Furthermore, Resini et al. [63] reported that the steam reforming of propene over a Pd-Cu/Al_2O_3 catalyst yielding CO and H_2, which could reduce stored NO_X as discussed previously, becomes significant at temperatures above 275 °C. These reports appear to be consistent with the data of Fig. 7, which suggests increased activity above 200 °C, reaching complete conversion of C_3H_6 at 350 °C. However, it is not possible to differentiate from this data between the amounts of C_3H_6 consumed during the direct reduction of NO_X and the amount converted to CO and H_2 via steam reforming. Finally, the results of Fig. 7B indicate that hydrocarbon slip may represent a problem for LNT catalyst operation lower temperatures, where NH_3 formation is favored, as will be discussed below.

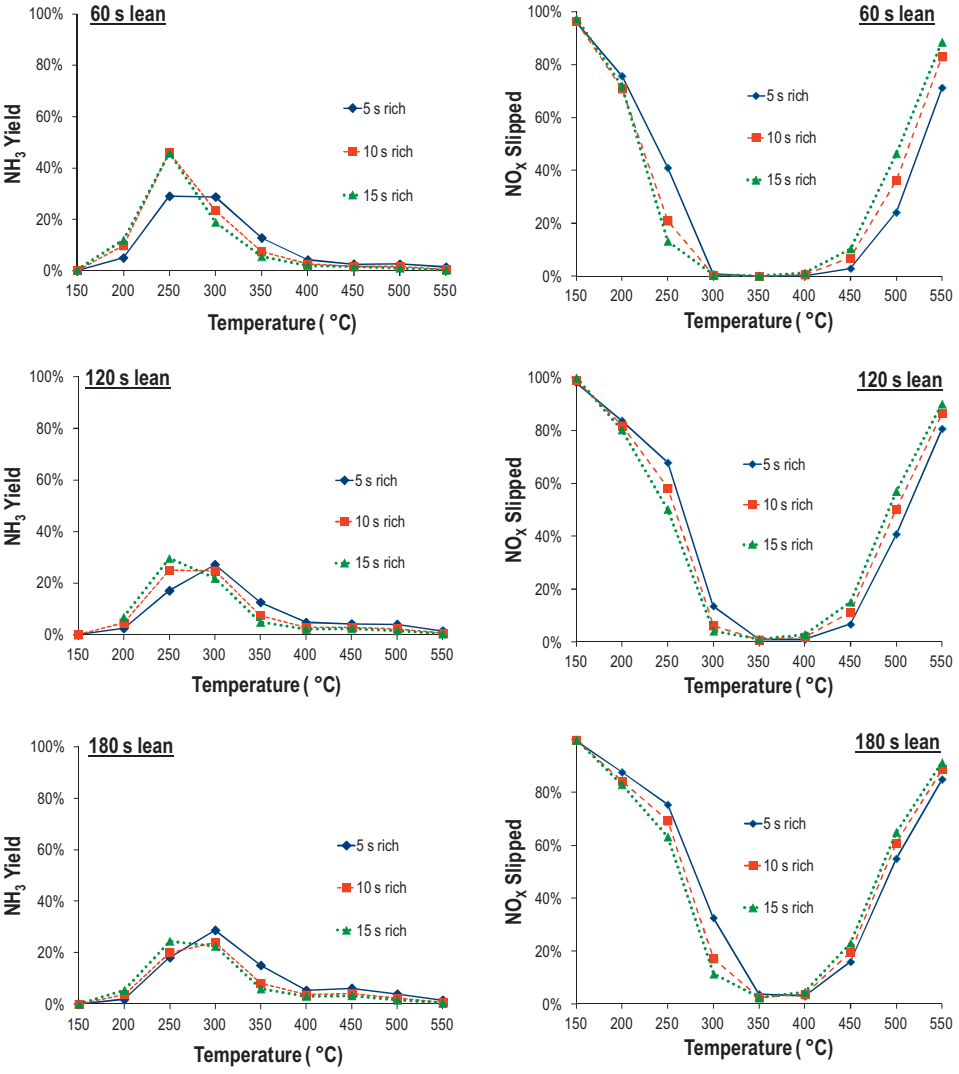

Fig. 9. Cycle averaged NH_3 yield and NO_X slip from the LNT catalyst as functions of temperature and lean/rich cycle timing.

3.4. NH_3 and N_2O formation

The results shown in Fig. 9 summarize the cycle-averaged NH_3 yield and NO_X slipped for the set of conditions considered in this investigation. This side by side comparison of NH_3 yield and NO_X slipped can be used as an indicator of the feasibility of an LNT-SCR configuration, since in this setup NH_3 stored downstream is used to reduce NO_X that "slips" from the LNT catalyst. Along these lines, the results shown in Fig. 9 demonstrate that it may be possible to select the appropriate temperature and cycling conditions to achieve the desired NO_X and NH_3 amount reaching the SCR catalyst. For example, if the length of the lean period is set at 60 s and the catalyst temperature is 250 °C, the length of the rich period pulse can be used to control the amount of NH_3 formed. When 10 or 15 s rich pulses are used, an NH_3 yield of 46% is observed, while the corresponding NO_X slip is 21% and 13% of the total NO_X fed, respectively. Since the SCR reaction requires a 1:1 NH_3:NO_X ratio, as shown in Eq. (9),

$$4NH_3 + 4NO + O_2 \rightarrow 4N_2 + 6H_2O \quad (9)$$

under these conditions the amount of NH_3 generated is theoretically twice the amount needed to operated a downstream SCR catalyst.

Consequently, the SCR catalyst could quickly become saturated with adsorbed NH_3 and significant concentrations of NH_3 instead of NO_X could appear in the final exhaust stream. Furthermore, this indicates that in this case the overall LNT-SCR configuration would operate with excess reducing agent due to longer than needed rich cycles. Not surprisingly then, when a 5 s rich cycle is used, the NO_X slip is approximately 41%, while the NH_3 yield is only 29%. In this case, more NO_X would be slipped from the catalyst system than NH_3. In this case, having a downstream SCR catalyst would be expected to improve the cycled averaged NO_X conversion, as previously observed by Lindholm et al. [22], but not all of the NO_X slipped from the LNT could be converted to N_2. In summary, the results shown in Fig. 9 can be used to identify the regions where controlling the NH_3 formation over the LNT catalyst would be expected to have the greatest impact on the LNT-SCR configuration, as more clearly shown in Fig. 10. This assumes that all of the NH_3 produced over the LNT catalyst can be stored on the SCR and subsequently used to reduce NO_X. In practice, complete storage and reaction of the NH_3 formed may not be possible and more NH_3 than stoichiometrically required might have to be formed over the LNT catalyst.

The results shown in Fig. 10 demonstrate one example (i.e., 60 s lean, 5 s rich) of how the NH_3 yield and NO_X slip profiles from this cycling investigation (Fig. 9) can be used to identify the region where controlling the NH_3 formation over the LNT would

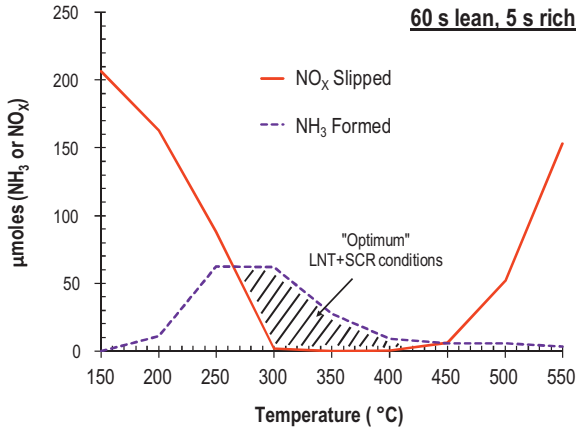

Fig. 10. Quantities (μmol) of NH_3 formed in comparison to the NO_X slipped for cycling conducted using 60 s lean, 5 s rich cycles.

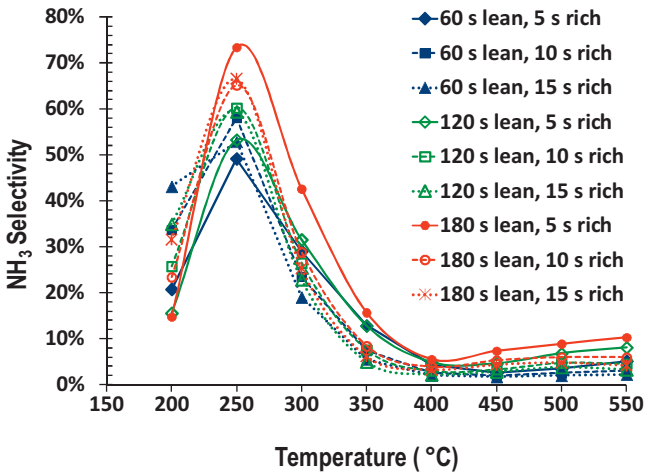

Fig. 11. Cycle averaged NH_3 selectivity obtained for the LNT catalyst as a function of temperature and lean/rich cycle timing.

be expected to have the greatest impact on performance if implemented in an LNT-SCR system. As shown, significant NO_X slip was observed below 250 °C and above 450 °C without sufficient NH_3 formation to allow for operation of a downstream SCR catalyst. On the other end of the spectrum, almost complete NO_X conversion is observed between 300 and 450 °C; in this case, the NH_3 formed over the LNT catalyst could represent a problem because very little NO_X remains to react with NH_3 over the SCR catalyst. Generally however, the region where balancing the amount of the NH_3 produced with the amount of NO_X slipped appears to be between 250 and 450 °C, which is very close to the region in which Lindholm et al. [22] reported increases in the cycled averaged NO_X conversion and N_2 selectivity for a close-coupled LNT-SCR system. The results of Fig. 10 also help explain the observations by Xu et al. [18] that LNT-SCR systems help mitigate catalyst deactivation due to aging. In that case, aging most likely increases the amount of NO_X slipped from the LNT, but this additional NO_X can be reduced by NH_3 formed over the LNT catalyst and stored on the downstream SCR component, as indicated by the comparison of the area between the two curves shown in Fig. 10. For this reason, the shaded region in Fig. 10 has been denoted as the "optimum" LNT ± SCR temperature region, since tuning the temperature and/or cycling conditions of the LNT within this temperature range can be expected to have a significant effect on the performance of a close-coupled LNT-SCR system.

Regardless of the length of the lean/rich cycle used, the NH_3 yield peaked at either 250 or 300 °C (Fig. 9), but NH_3 selectivity always reached a maximum at 250 °C, as shown in Fig. 11. The NH_3 selectivities measured at 250 °C are in excellent agreement with previously reported results by Ren and Harold [25] over a similar series of catalysts even though in their case H_2 was used as the reducing agent and CO_2 and H_2O were not simultaneously present in the feed. In contrast, below 250 °C, Ren and Harold [25] reported significantly higher NH_3 selectivities than in our case most likely due to the use of H_2 and its higher reduction potential over CO for temperatures below 250 °C [58,64]. Furthermore, the narrow NH_3 selectivity maximum at 250 °C, for a variety of cycle timing and reductant concentration conditions, clearly illustrates that the selectivity to NH_3 is primarily controlled by the reaction temperature over the LNT catalyst used. At temperatures below 250 °C, the slow formation of surface isocyanates and the low rate of the WGS reaction, which represent the two most likely pathways to NH_3 formation when CO is used as a reductant [24,32,37,50,65], can account for the low NH_3 yields.

Cycle-averaged N_2O yield and selectivity are shown as functions of temperature and cycle timing in Fig. 12. The results indicate that the N_2O yield shows a maximum at approximately the same temperature range as the NH_3 yield (i.e., 250–300 °C). As a result, N_2O production will be an issue if the LNT catalyst operates under the most favorable conditions for NH_3 production. In a recent publication however, Wang and Crocker [19] demonstrated that N_2O reduction over a downstream Cu-chabazite SCR catalyst could significantly reduce the amount of N_2O ultimately present in the

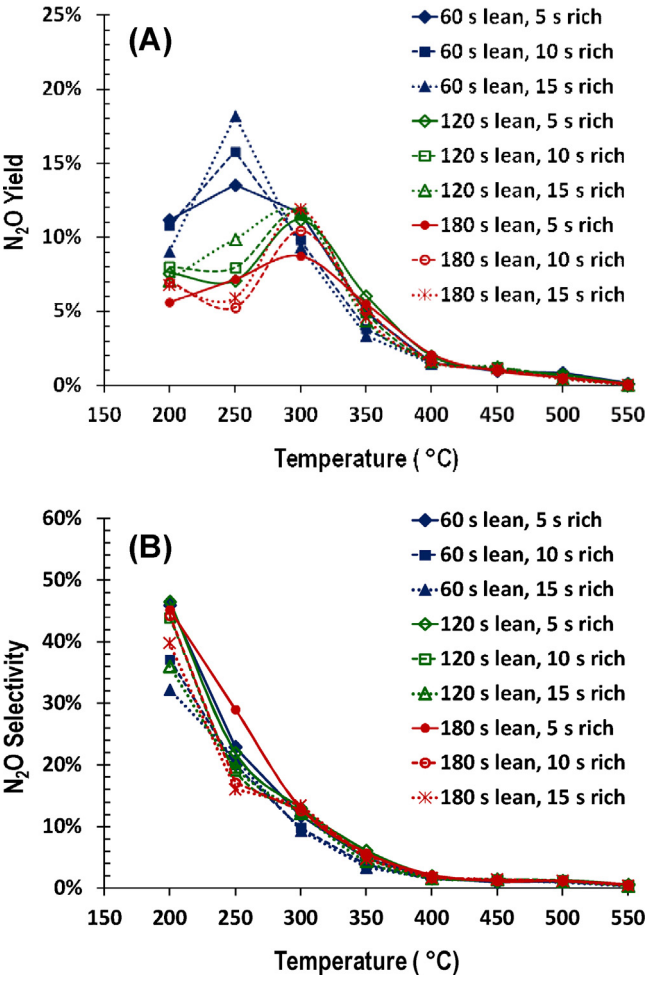

Fig. 12. Cycle averaged N_2O yield (A) and selectivity (B) obtained for the LNT catalyst as functions of temperature and lean/rich cycle timing.

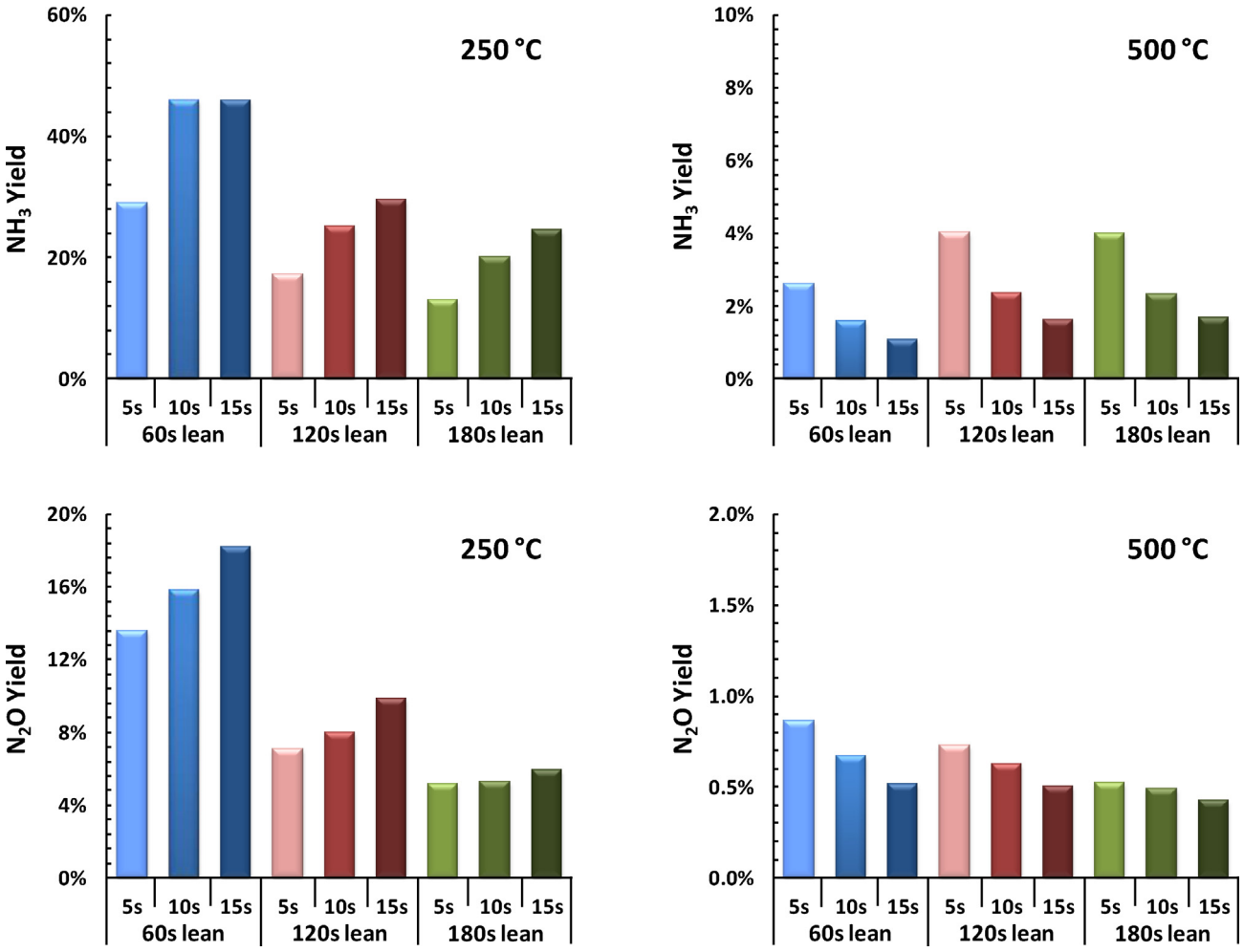

Fig. 13. Cycle averaged NH_3 and N_2O yields obtained for the LNT catalyst for different lean/rich cycle timing protocols at 250 and 500 °C.

exhaust of the overall after-treatment system; in their case, complete reduction of N_2O was reported at 315, 350 and 450 °C when H_2, NH_3 and CO, respectively, were used as the reducing agents. Furthermore, Wang and Crocker [19] reported significant decreases N_2O formation by 225 °C in an LNT-SCR configuration and complete removal by 275 °C. Consequently, one can conclude that the presence of a downstream SCR catalyst will significantly reduce the amount of N_2O slipped from the LNT catalyst at temperatures above 250 °C, but N_2O slip will still be a problem at temperatures below 250 °C.

In comparison to NH_3 selectivity, the selectivity to N_2O did not exhibit a maximum but instead it decreased monotonically as the temperature was increased (Fig. 12B). Once again, changes in the lean/rich cycle timing had a relatively small impact on the N_2O selectivity, in agreement with the results discussed above for the NH_3 selectivity, further supporting the conclusion that the predominant factor controlling NH_3 and N_2O selectivity over the LNT catalyst is the operating temperature.

Finally, the NH_3 and N_2O yields can be affected by the NO_X storage–reduction regime under which cycling is conducted. For example, the results shown in Fig. 13 depict two limiting cases for the NH_3 and N_2O yields. The cycle averaged NO_X conversions observed under these conditions are shown in Fig. 5. As previously discussed, the NO_X release and/or reduction rates were slower at 250 °C; therefore, longer, lower reductant concentration rich doses resulted in increased overall NO_X conversions. The amount of NO_X stored by the LNT catalyst at 250 °C also increased with the length of the rich cycle, with the 60 s lean/5 s rich and 60 s lean/15 s rich combinations resulting in 185 and 202 μmol of stored NO_X, respectively. As seen in Fig. 13, extending the length of the rich cycle also resulted in higher NH_3 and N_2O yields even though the reductant concentrations were lower in this case. Initially this result appears to contradict previous observations by Pihl et al. [48], where higher reductant concentrations resulted in increased NH_3 and N_2O yields. However, one has to consider that at lower temperatures the product distribution is significantly affected by the NO_X release and reduction rates in addition to the reductant concentration. At 250 °C for example, the increased NH_3 and N_2O yields can be attributed to a combination of increased NO_X conversion, which is affected by the length of the rich cycle, and constant selectivities to NH_3 and N_2O, which are almost independent of the length of the rich cycling duration (Figs. 11 and 12B). As a result, if the NO_X conversion and the amount of NO_X stored increase without a significant change in the product selectivities, the yield to those products increases as well. Alternatively at 500 °C, the higher reductant concentrations used during shorter rich cycles results in both higher NO_X conversions and higher NH_3 and N_2O yields, consistent with the results reported by Pihl et al. [48]. In this case, the NO_X stored on the LNT catalyst is released very quickly and high concentrations of reductant are needed to reduce all of the NO_X released. The amount of NO_X stored is also not affected by the length of the rich cycle, since the catalyst regeneration is very fast.

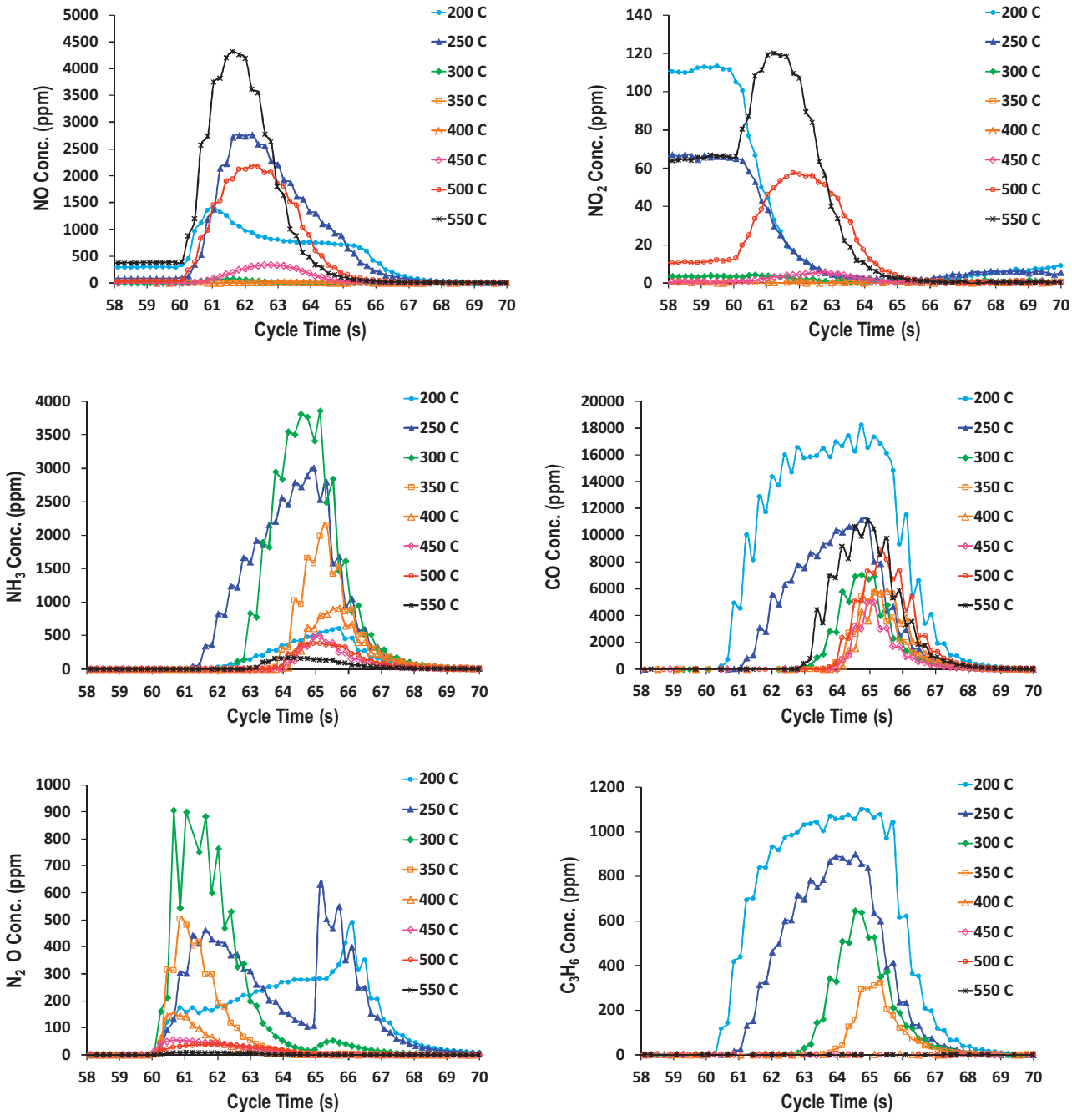

Fig. 14. LNT reactor effluent profiles for NO, NO_2, NH_3, CO, N_2O and C_3H_6 observed during a 5 s rich cycle following a 60 s lean cycle at different temperatures.

At this point, it is important to differentiate between regeneration limited conditions (e.g., ≤250–300 °C) and storage limited conditions (e.g., ≥450 °C), as previously discussed by Breen and Burch [53,55], because the rates of storage and regeneration have major implications on the observed catalytic performance for the production of NH_3, as indicated by our results. At low temperatures when NO_X release and regeneration are limiting, a longer, lower concentration rich cycle results in higher NO_X conversion than a shorter, higher concentration rich cycle because extending the length of rich cycle is critical for achieving more complete regeneration. In this case, despite the lower selectivity to NH_3, more NH_3 is actually produced because of higher NO_X conversions. At higher temperatures, this is no longer the case and higher concentration, short rich cycles, results in both higher NH_3 yield and selectivity, as previously reported by others [48,64].

3.5. Reactor effluent profiles

Concentration profiles for NO, NO_2, NH_3, CO, N_2O and C_3H_6 observed downstream of the LNT catalyst during a 5 s rich cycle following a 60 s lean cycle are shown for different temperatures in Fig. 14. As it becomes apparent from the results, these profiles vary significantly with temperature. For both NO and NO_2, for example, at temperatures above 450 °C maxima in the effluent concentrations are observed within the first 1–2 s following the switch to rich conditions. As previously reported [43,44], the reason for this

behavior is that NO_X is released much faster than it is reduced. At 550 °C, the maximum in the total NO_X concentration approached 4500 ppm, which is actually 9 times higher than the total NO_X concentration present in the feed. The NO and NO_2 profiles just prior to the switch to rich conditions at 60 s also demonstrate the poor storage capacity of the LNT at this temperature, since the NO_X concentration has already reached the feed concentration. At all other temperatures, with the exception of 200 °C, where storage is significantly limited, very low breakthrough of NO_X is observed prior to the onset of the rich period. Significant concentrations of NO_X are also observed during the rich cycle downstream of the LNT catalyst in the lower temperature range (i.e., 200–300 °C). In this case however, the maxima are lower and are more evenly distributed during the entire rich cycle and even extend in to the first 1–2 s of the subsequent lean cycle. This behavior can be attributed to the lower reduction activity of the LNT catalyst at these temperatures.

The appearance of NH_3 downstream of the LNT catalyst did not coincide with the onset of the rich cycle. Instead, a delay was observed at all temperatures examined; in fact, for temperatures above 350 °C, no NH_3 was observed until approximately 4 s into the 5 s rich cycle. This delay in NH_3 breakthrough has previously been attributed to NH_3 decomposition and oxidation and/or reaction with stored nitrites/nitrates as the NH_3 propagates through the catalyst bed [32,35,48,51,64]. Since higher temperatures favor these NH_3 reactions, especially for catalysts containing significant amount of OSC as in this case, the delay increases with reaction temperature. The CO concentration profiles closely matched the behavior observed for NH_3, with the exception of the lower temperature studied (200 °C), where apparently no significant CO-NO_X reaction takes place. The overall amount of CO in the LNT effluent stream reaches a minimum between 350 and 400 °C and then begins to increase as the temperature is further raised. The 350–400 °C temperature range represents the optimum operating temperature for this catalyst, where the amount of reductants fed most closely matches the amount of NO_X stored. At higher temperatures (>450 °C), the NO_X storage capacity of the LNT catalyst is reduced and as a result the reduction process becomes unbalanced during the rich cycle.

The C_3H_6 concentration profiles closely match those of CO at temperatures below 350 °C, which is consistent with results previously reported by Abdulhamid et al. [58] for H_2, CO and C_3H_6 at these temperatures. Above 350 °C, no C_3H_6 was observed in the effluent from the LNT catalyst. In contrast, CH_4 formation was observed starting at 350 °C, although the amount of CH_4 produced was relatively low. For example, the maximum CH_4 concentration did not exceed 150 ppm for any condition, yielding a cycled averaged concentration below 6 ppm. Hydrocarbon yields and selectivities can be rationalized via a complex network of parallel reactions incorporating oxidation, reforming and hydrogenolysis steps. The final concentration observed depends on the relative rates of these reactions, which change significantly with temperature and a detailed analysis of this network is beyond the scope of the current manuscript.

Finally, the N_2O profiles (Fig. 14) indicate the presence of N_2O in the effluent immediately after the transition from lean to rich conditions. At lower temperatures (i.e., ≤300 °C) an additional period of increased N_2O production was also observed during the transition from rich back to lean conditions. Results previously reported by Breen et al. [53] also showed two periods of N_2O production at 250 °C, but not 350 °C, in agreement with our results. In general, N_2O formation is believed to occur over LNT catalysts when low H_2/NO_X ratios are present on the catalyst surface, frequently associated with transition from lean to rich environments [19,44–46,53,58]. At lower temperatures, where the N_2O generation is especially pronounced, NO dissociation occurs slowly and N_2O formation is favored through coupling of an adsorbed N and NO adatom, especially in the absence of high H_2 concentrations [53]. Conversely, NH_3 formation is favored at high H/NO_X ratios, which are more likely to be present as regeneration proceeds in later stages of the rich cycle [44]. The NH_3 and N_2O profiles shown in Fig. 14 are consistent with these previous postulations, with the production of N_2O and NH_3 generally being mutually exclusive. An alternative pathway for the production of N_2O during the rich to lean transition could be the reaction of residual surface isocyanates (NCO) with NO or O_2. We have previously reported the presence of surface NCO species during cycling studies over a model LNT catalyst even in the presence of H_2O at 250 °C [24] and have shown along with others [61] that these species can react with NO or O_2, yielding N_2O. The surface concentration of isocyanates is significantly reduced at temperatures above 300 °C, which coincides with the disappearance of N_2O during the rich to lean transition in the profiles of Fig. 14, providing further support to the hypothesis that an isocyanate-based reaction mechanism may be responsible for this second period of N_2O production.

4. Conclusions

The results of the activity measurements performed in this study over a commercial catalyst and realistic lean/rich cycling conditions indicate the presence of two distinctly different regimes. At temperatures below 300 °C, NO_X release and subsequent reduction were slow processes. Therefore, longer, lower concentration rich pulses result in increased cycle averaged NO_X conversions. For example, extending the rich cycle from 5 to 15 s at 250 °C, while holding the overall reductant amount constant, resulted in an increase in cycle averaged NO_X conversion from approximately 59 to 87%, respectively. At temperatures above 450 °C, the opposite is true. Under these conditions, NO_X release and reduction occurs rapidly and shorter, higher concentration rich pulses are needed to achieve high NO_X conversions. For example, rich cycles of 5 to 15 s at 500 °C – once again, with a constant overall reductant amount – resulted in cycle averaged NO_X conversions of approximately 76 and 54%, respectively. The selectivities to NH_3 and N_2O are primarily functions of temperature and are higher at lower temperatures. The effect of cycle timing and reductant concentrations was of secondary importance on these selectivities. NH_3 and N_2O yields however, are significantly affected by the cycling timing parameters, since these strongly affect NO_X conversion as indicated above. The effects of cycling parameters are much less pronounced around the optimum operating temperature (i.e., 350–400 °C) of the LNT catalyst indicating that the maximum in NO_X conversion observed under these conditions is fairly robust. Finally, concerted control of NH_3 generation by varying the lean/rich cycle timing was demonstrated. The most significant effects, in terms of both NO_X conversion and NH_3 yield, were observed either by extending the rich cycle at lower temperatures (i.e., reduction limiting regime) or by shortening the rich cycle at higher temperatures (i.e., storage limiting regime), with the greatest impact occurring between 250 and 450 °C. In both cases, NH_3/NO_X ratios close to the stoichiometric one could be obtained at the effluent of the LNT, demonstrating the potential for extending the region of operation with the utilization of a coupled LNT-SCR system. N_2O yields however, also increased with NH_3 yields, especially at low temperatures, indicating that an efficient LNT-SCR configuration will also need to covert N_2O downstream of the LNT catalyst.

Acknowledgements

A portion of this work was sponsored by the U.S. Department of Energy, Office of Energy Efficiency and Renewable Energy,

Vehicle Technologies Program. The authors at ORNL thank program managers Ken Howden and Gurpreet Singh for their support. Additionally, the authors would like to acknowledge the contributions of Wei Li of General Motors and Davion Clark of Umicore for discussions and guidance in this portion of our research. This manuscript has been co-authored by UT-Battelle, LLC, under Contract No. DE-AC05-00OR22725 with the U.S. Department of Energy. The United States Government retains and the publisher, by accepting the article for publication, acknowledges that the United States Government retains a non-exclusive, paid-up, irrevocable, worldwide license to publish or reproduce the published form of this manuscript, or allow others to do so, for United States Government purposes.

References

[1] S. Roy, A. Baiker, Chemical Reviews 109 (2009) 4054.
[2] P.L.T. Gabrielsson, Topics in Catalysis 28 (2004) 177.
[3] J.R. Theis, E. Gulari, (2006-01-0210), Society of Automotive Engineers (SAE) (2006).
[4] R. Snow, D. Dobson, R. Hammerle, S. Katare, (2007-01-0469), Society of Automotive Engineers (SAE) (2007).
[5] L. Xu, R. Mccabe, W. Ruona, G. Cavataio, (2009-01-0285), Society of Automotive Engineers (SAE) (2009).
[6] L. Xu, R. Mccabe, M. Dearth, W. Ruona, (2010-01-0305), Society of Automotive Engineers (SAE) (2010).
[7] H. Shinjoh, N. Takahashi, K. Yokota, Topics in Catalysis 42–43 (2007) 215.
[8] T. Nakatsuji, M. Matsubara, J. Rouistenmäki, N. Sato, H. Ohno, Applied Catalysis B: Environmental 77 (2007) 190.
[9] E. Corbos, M. Haneda, X. Courtois, P. Marecot, D. Duprez, H. Hamada, Catalysis Communications 10 (2008) 137.
[10] E.C. Corbos, M. Haneda, X. Courtois, P. Marecot, D. Duprez, H. Hamada, Applied Catalysis A: General 365 (2009) 187.
[11] D. Chatterjee, P. Kočí, V. Schmeißer, M. Marek, M. Weibel, B. Krutzsch, Catalysis Today 151 (2010) 395.
[12] P. Forzatti, L. Lietti, I. Nova, E. Tronconi, Catalysis Today 151 (2010) 202.
[13] R. Bonzi, L. Lietti, L. Castoldi, P. Forzatti, Catalysis Today 151 (2010) 376.
[14] P. Forzatti, L. Lietti, Catalysis Today 155 (2010) 131.
[15] L. Castoldi, R. Bonzi, L. Lietti, P. Forzatti, S. Morandi, G. Ghiotti, S. Dzwigaj, Journal of Catalysis 282 (2011) 128.
[16] Y. Liu, M.P. Harold, D. Luss, Applied Catalysis B: Environmental 121–122 (2012) 239.
[17] J. Wang, Y. Ji, Z. He, M. Crocker, M. Dearth, R.W. McCabe, Applied Catalysis B: Environmental 111–112 (2012) 562.
[18] L. Xu, R.W. McCabe, Catalysis Today 184 (2012) 83.
[19] J. Wang, M. Crocker, Catalysis Letters 142 (2012) 1167.
[20] H.S. Gandhi, J.V. Cavataio, R.H. Hammerle, Y. Cheng, U.S.P. 7332135 (2002).
[21] H.S. Gandhi, J.V. Cavataio, R.H. Hammerle, Y. Cheng, U.S.P. 7485273 (2009).
[22] A. Lindholm, H. Sjövall, L. Olsson, Applied Catalysis B: Environmental 98 (2010) 112.
[23] J.R. Theis, M. Dearth, R. McCabe, (2011-01-0305), Society of Automotive Engineers (SAE) (2011).
[24] C.D. DiGiulio, V.G. Komvokis, M.D. Amiridis, Catalysis Today 184 (2012) 8.
[25] Y. Ren, M.P. Harold, ACS Catalysis 1 (2011) 969.
[26] V.I. Parvulescu, P. Grange, B. Delmon, Catalysis Today 46 (1998) 233.
[27] A. Grossale, I. Nova, E. Tronconi, Catalysis Today 136 (2008) 18.
[28] S.J. Schmieg, S.H. Oh, C.H. Kim, D.B. Brown, J.H. Lee, C.H.F. Peden, D.H. Kim, Catalysis Today 184 (2012) 252.
[29] J. Baik, S. Yim, I. Nam, Y. Mok, J. Lee, B. Cho, S. Oh, Topics in Catalysis 30/31 (2004) 37.
[30] J.H. Kwak, D. Tran, S.D. Burton, J. Szanyi, J.H. Lee, C.H.F. Peden, Journal of Catalysis 287 (2012) 203.
[31] S.S. Mulla, S.S. Chaugule, a. Yezerets, N.W. Currier, W.N. Delgass, F.H. Ribeiro, Catalysis Today 136 (2008) 136.
[32] L. Cumaranatunge, S. Mulla, A. Yezerets, N. Currier, W. Delgass, F. Ribeiro, Journal of Catalysis 246 (2007) 29.
[33] A. Kumar, M.P. Harold, V. Balakotaiah, Journal of Catalysis 270 (2010) 214.
[34] R.D. Clayton, M.P. Harold, V. Balakotaiah, Applied Catalysis B: Environmental 84 (2008) 616.
[35] L. Lietti, I. Nova, P. Forzatti, Journal of Catalysis 257 (2008) 270.
[36] I. Nova, L. Lietti, P. Forzatti, Catalysis Today 136 (2008) 128.
[37] I. Nova, L. Lietti, P. Forzatti, F. Prinetto, G. Ghiotti, Catalysis Today 151 (2010) 330.
[38] http://www.cleers.org/ (2012).
[39] J.-S. Choi, W.P. Partridge, M.J. Lance, L.R. Walker, J.A. Pihl, T.J. Toops, C.E.a. Finney, C.S. Daw, Catalysis Today 151 (2010) 354.
[40] J.-S. Choi, W.P. Partridge, J.A. Pihl, M.-Y. Kim, P. Kočí, C.S. Daw, Catalysis Today 184 (2012) 20.
[41] M. Boaro, C. de Leitenburg, G. Dolcetti, A. Trovarelli, Journal of Catalysis 193 (2000) 338.
[42] W. Li, General Motors "Personal Communication" (2012).
[43] Y. Ji, J.-S. Choi, T.J. Toops, M. Crocker, M. Naseri, Catalysis Today 136 (2008) 146.
[44] Y. Ji, V. Easterling, U. Graham, C. Fisk, M. Crocker, J.-S. Choi, Applied Catalysis B: Environmental 103 (2011) 413.
[45] W.S. Epling, A. Yezerets, N.W. Currier, Applied Catalysis B: Environmental 74 (2007) 117.
[46] U. Elizundia, D. Duraiswami, B. Pereda-Ayo, R. López-Fonseca, J.R. González-Velasco, Catalysis Today 176 (2011) 324.
[47] R.D. Clayton, M.P. Harold, V. Balakotaiah, Applied Catalysis B: Environmental 81 (2008) 161.
[48] J.A. Pihl, J.E. Parks, C.S. Daw, T.W. Root, (2006-01-3441), Society of Automotive Engineers (SAE) (2006).
[49] J.R. Theis, J.A. Ura, J.J. Li, G.G. Surnilla, J.M. Roth, C.T.G. Jr, (2003-01-1159), Society of Automotive Engineers (SAE) (2003).
[50] I. Nova, L. Lietti, L. Castoldi, E. Tronconi, P. Forzatti, Journal of Catalysis 239 (2006) 244.
[51] B. Pereda-Ayo, J.R. González-Velasco, R. Burch, C. Hardacre, S. Chansai, Journal of Catalysis 285 (2012) 177.
[52] P. Forzatti, L. Lietti, I. Nova, S. Morandi, F. Prinetto, G. Ghiotti, Journal of Catalysis 274 (2010) 163.
[53] J.P. Breen, R. Burch, C. Fontaine-Gautrelet, C. Hardacre, C. Rioche, Applied Catalysis B: Environmental 81 (2008) 150.
[54] Y. Ji, T.J. Toops, M. Crocker, Catalysis Letters 119 (2007) 257.
[55] J.P. Breen, C. Rioche, R. Burch, C. Hardacre, F.C. Meunier, Applied Catalysis B: Environmental 72 (2007) 178.
[56] M. AL-Harbi, W.S. Epling, Catalysis Today 151 (2010) 347.
[57] K.S. Kabin, R.L. Muncrief, M.P. Harold, Catalysis Today 96 (2004) 79.
[58] H. Abdulhamid, E. Fridell, M. Skoglundh, Topics in Catalysis 30/31 (2004) 161.
[59] C.M.L. Scholz, B.H.W. Maes, M.H.J.M. de Croon, J.C. Schouten, Applied Catalysis A: General 332 (2007) 1.
[60] I. Nova, L. Lietti, P. Forzatti, F. Frola, F. Prinetto, G. Ghiotti, Topics in Catalysis 52 (2009) 1757.
[61] J.-Y. Luo, W.S. Epling, Applied Catalysis B: Environmental 97 (2010) 236.
[62] J. Theis, H. Jen, R. Mccabe, M. Sharma, V. Balakotaiah, M.P. Harold, (2006-01-1067), Society of Automotive Engineers (SAE) (2006).
[63] C. Resini, L. Arrighi, M. Concepcionherreradelgado, M. Angeleslarrubiavargas, L. Alemany, P. Riani, S. Berardinelli, R. Marazza, G. Busca, International Journal of Hydrogen Energy 31 (2006) 13.
[64] J. Wang, Y. Ji, V. Easterling, M. Crocker, M. Dearth, R.W. McCabe, Catalysis Today 175 (2011) 83.
[65] T. Szailer, J. Kwak, D. Kim, J. Hanson, C. Peden, J. Szanyi, Journal of Catalysis 239 (2006) 51.